2013

# Intrinsic Properties of Fe-Substituted L10Magnets

Priyanka Manchanda
*LMN Institute of Information Technology*, priyanka.manchanda@vanderbilt.edu

Pankaj Kumar
*Kendriya Vidhyalaya*, panksamrat@gmail.com

Arti Kashyap
*LMN Institute of Information Technology*, akashyap@lnmiit.ac.in

M. J. Lucis
*University of Nebraska-Lincoln*

Jeffrey E. Shield
*University of Nebraska-Lincoln*, jshield@unl.edu

*See next page for additional authors*

# Intrinsic Properties of Fe-Substituted $L1_0$ Magnets

P. Manchanda[1,2], Pankaj Kumar[1,2], A. Kashyap[1], M. J. Lucis[3], J. E. Shield[3], A. Mubarok[4], J. I. Goldstein[4], S. Constantinides[5], K. Barmak[6], L. H. Lewis[7], D. J. Sellmyer[2], and R. Skomski[2]

[1]School of Basic Sciences, Indian Institute of Technology, Mandi, Himachal Pradesh, India
[2]Department of Physics and Astronomy and NCMN, University of Nebraska, Lincoln, NE 68588 USA
[3]Department of Mechanical and Materials Engineering, University of Nebraska, Lincoln, NE 68588 USA
[4]Department of Mechanical and Industrial Engineering, University of Massachusetts, Amherst, MA 01003 USA
[5]Arnold Magnetic Technologies, Rochester, NY 14625 USA
[6]Department of Applied Physics and Applied Mathematics, Columbia University, New York, NY 10027 USA
[7]Department of Chemical Engineering, Northeastern University, Boston, MA 02115 USA

**First-principle supercell calculations are used to determine how $3d$ elemental additions, especially Fe additions, modify the magnetization, exchange and anisotropy of $L1_0$-ordered ferromagnets. Calculations are performed using the VASP code and partially involve configurational averaging over site disorder. Three isostructural systems are investigated: Fe-Co-Pt, Mn-Al-Fe, and transition metal-doped Fe-Ni. In all three systems the iron strongly influences the magnetic properties of these compounds, but the specific effect depends on the host. In CoPt(Fe) iron enhances the magnetization, with subtle changes in the magnetic moments that depend on the distribution of the Fe and Co atoms. The addition of Fe to MnAl is detrimental to the magnetization, because it creates antiferromagnetic exchange interactions, but it enhances the magnetic anisotropy. The replacement of 50% of Mn by Fe in $\mathrm{MnFeAl_2}$ enhances the anisotropy from 1.77 to 2.5 $\mathrm{MJ/m^3}$. Further, the substitution of light $3d$ elements such as Ti, V, Cr into $L1_0$-ordered FeNi is shown to substantially reduce the magnetization.**

***Index Terms*—Density-functional theory, magnetic alloys, magnetic moment, permanent magnets.**

## I. Introduction

IRON donates a low raw materials cost and a high magnetization, and is therefore a preferred constituent for permanent magnets. However, the effect of Fe is sometimes detrimental to the magnetic properties; achieving a high magnetocrystalline anisotropy in Fe-containing alloys and compounds is a demanding challenge. Here our focus is clarifying the intrinsic properties of three Fe-substituted $L1_0$-ordered alloys with particular emphasis on the magnetic moment and the magnetocrystalline anisotropy constants. These systems are physically very different but all crystallize in the chemically-ordered tetragonal $L1_0$ structure [1]–[6]. The most general $L1_0$ structure, Fig. 1(a), has the composition $ABC_2$ [7], but in many simple $L1_0$ alloys, $A = B$, leading to equiatomic net compositions such as CoPt, FePt, and MnAl. Compared to a large variety of experimental and theoretical papers on ordered $3d/4d$ and $3d/5d$ alloys [7], [8], chemically-disordered alloys are less well-investigated, especially from a theoretical point of view. From the theoretical point of view, the coherent potential approximation (CPA) has been used to investigate various substitutions in $L1_0$ compounds containing Pt and Pd [9], [10].

In this paper we discuss the magnetic properties of three alloy compositions calculated using density functional theory. First, we investigate chemically-ordered and -disordered CoPt(Fe) to explore the prospect of reducing raw materials costs by substituting Fe and Co for Pt. The uniaxial magnetocrystalline anisotropy gradually decreases and reaches zero in cubic $L2_0$-ordered $\mathrm{Fe_3Pt}$. However, in the intermediate compositional regime, good magnetic properties have been achieved, such as magnetizations of up to 1.78 T and coercivities of up to 2.52 T [11], [12].

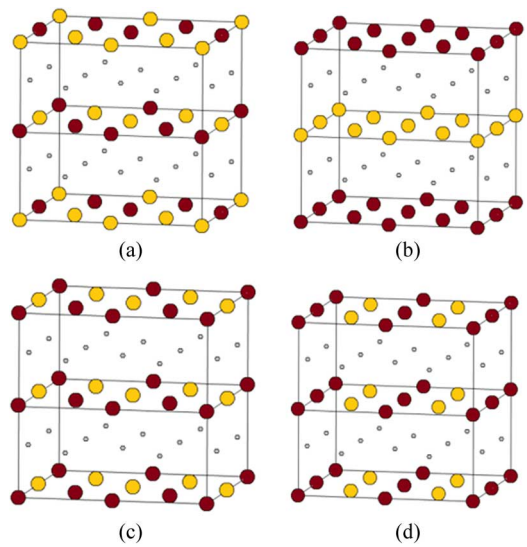


Fig. 1. Structures of some ordered $L1_0$-based Fe-Co-Pt alloys: (a) most general $L1_0$ structure (b) layered structures, (c) "striped" configuration and (d) "antistriped" configuration.

Second, we consider Fe substitutions in $\tau$-phase MnAl, which is one of the few ferromagnetic manganese-based alloys [13], [14] with appreciable intrinsic magnetic properties ($\mu_o M_s = 0.75$ T, $K_1 = 1.7\ \mathrm{MJ/m^3}$) [6]. These values are somewhat inferior to the intrinsic properties of FePt and CoPt, and small carbon additions are necessary to improve the stability of the $L1_0$-phase [15], [16], but both Mn and Al are inexpensive and readily available.

Manuscript received January 30, 2013; revised March 26, 2013; accepted April 28, 2013. Date of publication May 06, 2013; date of current version September 20, 2013. Corresponding author: L. Lewis (e-mail: lhlewis@neu.edu).

Color versions of one or more of the figures in this paper are available online at http://ieeexplore.ieee.org.

Digital Object Identifier 10.1109/TMAG.2013.2261821

The third issue explored here is the effect of $3d$ transition metal substitution in $L1_0$-type FeNi. The $L1_0$-type FeNi, known as tetrataenite, naturally occurs in meteorites but requires cooling times in excess of one million years to form the chemically-ordered phase [17], [18]. The tetrataenite phase forms from disordered fcc FeNi below 320°C or as part of a spinodal reaction as shown in the modern Fe-Ni binary phase diagram [19]. $L1_0$-ordered FeNi or tetrataenite can be produced metastably by electron and neutron bombardment and exhibits a fairly large magnetic anisotropy ($K_1 = 0.32$ MJ/cm$^3$, $K_2 = 0.23$ MJ/cm$^3$) [20]–[23]. Tetrataenite with appropriate alloying additions is now under exploration for advanced permanent magnet applications [23].

## II. Calculation

Calculations of the influence of Fe on the magnetic properties of $L1_0$-type CoPt(Fe), MnAl(Fe) and FeNi are performed using the frozen-core full-potential projected augmented wave (PAW) method [24], as implemented in the Vienna *ab-initio* simulation package (VASP) and based on density functional theory. The PAW method is basically an all-electron technique, with the advantage that it is almost as fast as the usual plane-wave pseudopotential method. The electronic exchange and correlation effects are described within the generalized-gradient approximation (GGA) using the functional proposed by Perdew *et al.* [25] and the spin interpolation proposed by Vosko *et al.* [26]. The GGA predicts the magnetic moments with a high accuracy, whereas the local spin-density approximation (LSDA) underestimates the magnetic moments of Fe, Co and Ni [28].

In our calculations the energy cutoff of the plane wave basis set is taken as 450 eV and total energy of the system is converged to $10^{-7}$ eV for all the considered structures, using Végard's Law based on the following experimental lattice constants: MnAl ($a = 3.93$ Å, $c = 3.56$ Å) [13], FePt ($a = 3.861$ Å and $c = 3.788$ Å) [35], CoPt ($a = 3.806$ Å and $c = 3.684$ Å) [29], FeNi ($a = c = 3.582$ Å) [30]. To ensure reasonable accuracy, all calculations use a $11 \times 11 \times 11$ mesh generating 126 $k$-points in the irreducible part of Brillouin Zone using the Monkhorst-pack scheme [27]. For some systems we have also performed magnetic-anisotropy calculations and then used 2197 $k$-points in the irreducible part of Brillouin Zone to ensure convergence.

## III. Results and Discussion

### A. Iron-Cobalt-Platinum

We have considered binary $L1_0$ alloys (FePt, CoPt), several chemically-ordered ternary $L1_0$-based alloys and disordered Fe-Co-Pt configurations. Fig. 1 shows the ordered ternary alloy structures, which have the composition $Fe_8Co_8Pt_{16}$. In these alloys Co occupies the regular sites in the ternary $L1_0$ structure (a), forms alternating layers with the stacking sequence Pt-Fe-Pt-Co (b), or forms stripes in each layer (c, d). The difference between Fig. 1(c) and (d) is that the stripes of (c) form vertical sequences with stacking Pt-Co-Pt-Co, whereas the antistriped alloy (d) has the stacking Pt-Fe-Pt-Co.

The chemically-disordered Fe-Co-Pt alloys are approximated by supercells with 32 atoms and have the nominal compositions

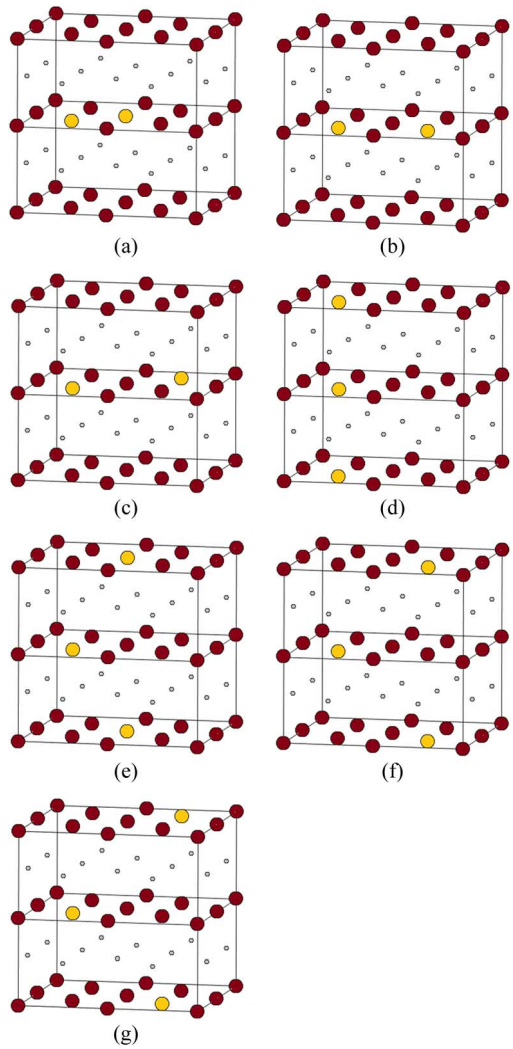


Fig. 2. Structures of some disordered $L1_0$-based $Fe_{14}Co_2Pt_{16}$ alloys.

$Fe_{15}CoPt_{16}$ ($x = 6.25\%$) and $Fe_{14}Co_2Pt_{16}$ ($x = 12.5\%$). In $Fe_{15}CoPt_{16}$, all Co sites are equivalent, because Co is assumed to substitute for one of the Fe atoms. In $Fe_{14}Co_2Pt_{16}$ ($x = 0.125$), there are 7 non-equivalent Co configurations, as shown in Fig. 2. Each of these configurations requires a separate first-principles calculation and the net moments $m_X$ ($X$ = Fe, Co, Pt, total) are then obtained by configurational averaging. Since some of the configurations are equivalent, the averaging over the 7 configurations requires specific weights of 4 (a), 2 (b), 1 (c), 1 (d), 4 (e), 2 (f) and 1. The sum of these weights is equal to 15, corresponding to $15 = 16 - 1$ supercell positions available for the second Co atom.

Fig. 3 shows the spin-resolved density of states (DOS) of the Fe, Co and Pt atoms in $Fe_{15}CoPt_{16}$. The majority spin bands are fully occupied for both Co and Fe, but the Fe minority spin band is shifted to higher energies relative to that of Co. This effect results in an increase of energy splitting between the majority and minority DOS. Correspondingly, the magnetic moment of the Fe atoms is larger than that of Co atoms.

Table I list the calculated atomic moments for the ferromagnetic Fe-Co-Pt alloys studied here. The moments of FePt and CoPt alloys are consistent with those reported in previous work

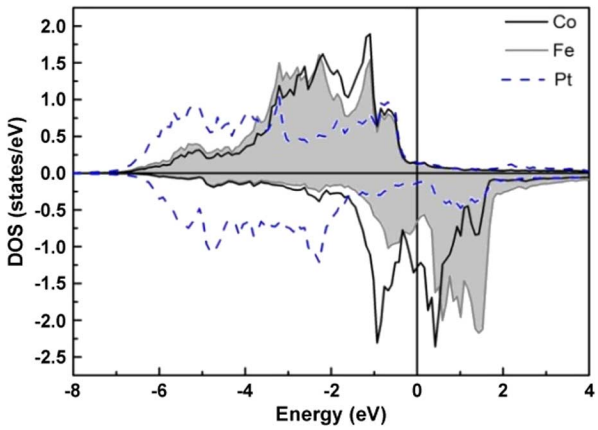


Fig. 3. Spin-polarized density of states of $Fe_{15}CoPt_{16}$ system. The gray area refers to the DOS of the Fe atoms.

TABLE I
MAGNETIC MOMENTS (IN $\mu_B$ PER ATOM) IN CHEMICALLY-ORDERED AND CHEMICALLY-DISORDERED FERROMAGNETIC Fe-Co-Pt ALLOYS

| System | <Co> | <Fe> | <Pt> | <*m*> |
|---|---|---|---|---|
| $Fe_{15}Co$-$Pt_{16}$ | 1.852 | 2.907 | 0.367 | 1.604 |
| $Fe_{14}Co_2$-$Pt_{16}$ | 1.857 | 2.919 | 0.372 | 1.579 |
| Ordered $Fe_8Co_8$-$Pt_{16}$ | 1.805 | 3.034 | 0.390 | 1.405 |
| Layered $Fe_8Co_8$-$Pt_{16}$ | 1.921 | 2.915 | 0.393 | 1.406 |
| "Striped" $Fe_8Co_8$-$Pt_{16}$ | 1.877 | 2.983 | 0.395 | 1.413 |
| "Antistriped" $Fe_8Co_8$-$Pt_{16}$ | 1.887 | 2.976 | 0.395 | 1.413 |
| Bulk-FePt | - | 2.916 | 0.339 | 1.628 |
| Bulk-CoPt | 1.847 | - | 0.403 | 1.125 |
| $Fe_2CoPt$ | 1.738 | 2.877 | 0.320 | 1.953 |
| $Fe_3Pt$ | | 2.805 | 0.330 | 2.186 |

[31]. Note that the spin state of perfectly chemically-ordered FePt has been subject to debate. Both antiferromagnetic [32] and ferromagnetic [33] ground-state predictions for perfectly chemically-ordered FePt were obtained, the latter using a GGA approach. According to Zhou *et al.* [34] ferromagnetism arises from exchange coupling between Fe and Pt. Our calculations yield a very weak ferromagnetic exchange and the energy difference is very small, 0.005 eV per atom, with the FM-AFM transition within the margin of error. In any case, the ground state of this system depends on the degree of chemical disorder and the tetragonal distortion [32], and there are indications that chemical disorder [7] or additions of Co [12], [36] or Fe are necessary to stabilize the ferromagnetic state. $Fe_2CoPt$ and $Fe_3Pt$ are examples of materials with very stable ferromagnetic moments (last two rows of Table I).

The Fe magnetic moments in chemically-ordered and layered $Fe_8Co_8Pt_{16}$ are 3.034 $\mu_B$ and 2.915 $\mu_B$, respectively, whereas the configurations of Fig. 1(c), (d) are intermediate between ordered and layered $Fe_8Co_8Pt_{16}$. The local magnetic moments of the Fe and Co atoms are dependent upon the bonding environment, and the Fe moment increases with the number of Co nearest neighbors. The local magnetic moments of the Fe atom are strongly environment-dependent. The small Pt moment of 0.3–0.4 $\mu_B$ is induced by the Fe and Co atoms, which is a well-known phenomenon.

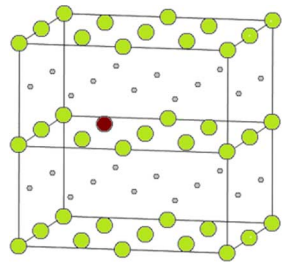

Fig. 4. Supercell used in 6.25% Fe substituted in MnAl alloys. Fe is shown in red, Mn in green and Pt in grey.

Our calculations confirm the basic trends of the magnetic moment found in earlier coherent-potential approximation (CPA) calculations on $Fe_{1-x}Co_xPt$ [9]. In particular, the total magnetization *decreases* with increasing Co content. This is because the $L1_0$ structure is a dense-packed structure that cannot be compared with bcc iron, where the Co additions provide $3d$ electrons to the majority band of the weakly ferromagnetic Fe (Slater-Pauling curve).

Note that the CPA is a single-site approximation, which ignores short-range order and cluster-localization effects [7]. The present supercell calculations, which go beyond CPA, allow accurate tracing of neighboring moments, but the corresponding corrections do not have a big effect on the net moment. Furthermore, the calculations become very cumbersome for higher Co concentrations, and little can be learned by considering large random-alloy supercells. In fact, since the CPA is a single-site approximation, cluster-localization effects are expected to be most pronounced for strong deviations from random disorder, as depicted in Fig. 1(b). Increasing the size of the supercell, which gives improved results for random solid solutions, is not meaningful or necessary here—by symmetry, the moments remain unchanged on increasing the unit cell size.

### *B. Manganese-Aluminum-Iron*

Fig. 4 shows the supercell that was used in our calculation for $Mn_{15}FeAl_{16}$, corresponding to the composition of 6.25 at.% Fe. For equiatomic $L1_0$ MnAl alloys, we obtain Mn and Al moments of 2.420 $\mu_B$ and $-0.061$ $\mu_B$, respectively. Additions of Fe reduce the magnetization of the alloy. For 6.25% Fe, the reduction is about 1.5%. $MnFeAl_2$ is antiferromagnetic, characterized by magnetic moments of Mn, Fe and Al of values 2.461 $\mu_B$, 1.899 $\mu_B$, and $-0.056$ $\mu_B$, respectively, which correspond to a net magnetization reduction of 10%. The calculated effect of Fe substitution on the magnetization of MnAl is consistent with preliminary experimental results that will be published in a separate paper. Fig. 5 shows the spin-resolved density of states (DOS) for the Fe-Mn-Al system.

Interestingly, we find that the Curie temperature of $L1_0$-type MnAl is determined by the exchange coupling *within* the Mn layers; only a very small ferromagnetic contribution is contributed by interlayer exchange mediated by the aluminum layers. By comparing the energies of various spin configurations we obtain an intralayer exchange of $J = 502$ K and

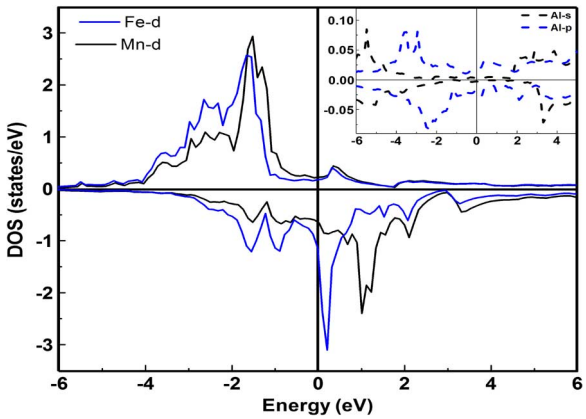


Fig. 5. Spin-polarized majority ($\uparrow$) and minority ($\downarrow$) $d$-band densities of states (DOS) of $MnFeAl_2$. The inset shows the $s$- and $p$-band DOS of Al.

an interlayer exchange of $J' = 73$ K, which translates into a Curie temperature prediction of 718 K, as compared to the experimental value of about 650 K. This strongly ferromagnetic intralayer exchange indicates that ferromagnetic exchange interactions are possible even for very short Mn-Mn distances. By contrast, the well-known Bethe-Slater-Néel curve suggests that large Mn-Mn distances are necessary to achieve ferromagnetic exchange. The substitution of Fe for Mn creates an antiferromagnetic intralayer exchange coupling, further reducing the overall magnetization below the above-mentioned values.

By contrast, Fe substitution enhances the magneto-crystalline anisotropy of $L1_0$-type MnAl. The calculated zero-temperature magnetic anisotropy of MnAl, $K_1 = 1.77$ MJ/m$^3$ [17.7 Mergs/cm$^3$], is consistent with previous experimental and theoretical results [37], [38]. The magnetic anisotropy for 6.25 at% substitution of Fe is 1.81 MJ/m$^3$ and that for 12.5 at% Fe is 1.9 MJ/m$^3$. For 50% Fe substitution, corresponding to $MnFeAl_2$, the zero-temperature anisotropy energy is 2.5 MJ/m$^3$.

### C. Transition-Metal-Substituted FeNi (Tetrataenite)

While $L1_0$-ordered FeNi (tetrataenite) is anticipated to possess high magnetization and high magnetocrystalline anisotropy, it exhibits a rather low chemical disorder-order temperature of 320°C and a very small atomic mobility of Fe and Ni at temperatures below the ordering temperature. These features make it very difficult to produce in the laboratory. However, ternary phase diagrams such as Fe-Ni-S [39] and processing experiments where tetrataenite forms in laboratory time scales [40] indicate that FeNi may be formed more rapidly. In particular, attainment of the chemically-ordered $L1_0$-type FeNi phase may be facilitated by the introduction of the lattice vacancies and/or alloying additions that provide phase stabilization. The question arises as to how these elemental or point defect additions might affect the intrinsic magnetic properties of FeNi. To address this question, preliminary computational exploration of elemental substitution of $3d$ transition metal in $L1_0$-ordered FeNi was carried out by replacing 50% of Ni by $3d$ transition metals. In particular, we have investigated the effect of $3d$ transition-metal (Ti, V, Cr, Mn, Fe, Co) substitutions on magnetization of FeNi as shown in Fig. 6.

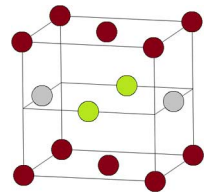

Fig. 6. Transition metal ($T$) substituted in FeNi. Fe is shown in red, Ni in grey and $T$ in green.

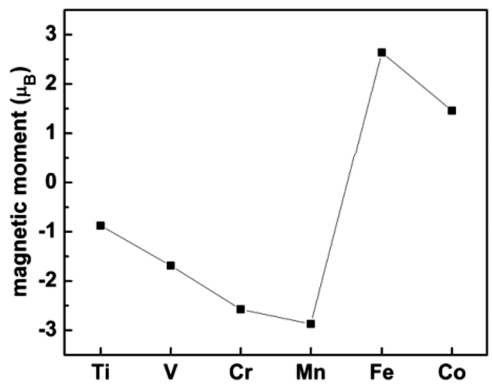


Fig. 7. The calculated magnetic moment of $3d$ transition metal ($T$) dopants on the Ni sites in $L1_0$-ordered FeNi. A negative sign corresponds to antiferromagnetic spin alignment.

Fig. 7 shows the calculated magnetic moment for $3d$ transition metal ($T$) substitutions dopants in FeNi. It is to be noted that Fe substitutions on the Ni site is most favorable for fostering a high moment. Antiferromagnetic spin alignment has been observed for Ti, V, Cr and Mn. For $L1_0$-ordered FeNi we find a strongly ferromagnetic Fe-Ni interlayer exchange coupling, in contrast to the very weak $3d$ interlayer coupling in found in isostructural MnAl and FePt. Transition-metal substitutions in FeNi also affect the zero-temperature magnetocrystalline anisotropy, which is 0.33 MJ/m$^3$ for $Fe_2NiTi$. By comparison, the calculated magnetic anisotropy energy in FeNi is 0.73 MJ/m$^3$; comparable with the experimental value provided by Néel (0.67 MJ/m$^3$) [22] and with earlier theoretical predictions [41], [42]. The effect of metalloid substitutions is under current investigation.

## IV. Conclusions

In summary, we have used supercell calculations to determine magnetic properties of $L1_0$-ordered Fe-Co-Pt, Mn-Al-Fe, and transition-metal-doped FeNi alloys. The Mn and Al moments in pure MnAl are 2.420 $\mu_B$ and $-0.061$ $\mu_B$ per atom, respectively, which means that the coupling between Mn and Al sublattices is antiferromagnetic. The calculated zero-temperature magnetic anisotropy energy is 1.77 MJ/m$^3$. The magnetic anisotropy energy increases as the concentration of Fe in MnAl alloys increases. For Fe-Co-Pt alloys, we have performed a configurational averaging for $Fe_{1-x}Co_xPt$ ($x < 0.15$) and considered a variety of chemically-ordered Fe-Co-Pt configurations. As a rule, the Fe and Co moments increase and decrease with increasing number of Fe-Co nearest neighbors, respectively. Our

results are important for the understanding of the magnetic moment of off-stoichiometric $L1_0$ alloys, as presently explored in permanent magnetism.

## ACKNOWLEDGMENT

This research was supported by ARPA-E REACT (ML, JES, LHL, JG, AM, KB and SC) and partially supported by NSF MRSEC (RS, JES), DST (PM, AK, PK), DOE (DJS), and ARPA-E Delaware (JES, DJS). Special recognition is provided to F. Pinkerton and E. Poirier of General Motors R. & D. Center for helpful discussions.

## REFERENCES

[1] L. Graf and A. Kussmann, "Zustandsdiagramm und magnetische Eigenschaften von Platin-Eisen-Legierungen," *Z Phys.*, vol. 36, pp. 544–551, 1935.

[2] D. J. Sellmyer, "Applied physics: Strong magnets by self assembly," *Nature*, vol. 420, pp. 374–375, Nov. 2002.

[3] H. Zeng, R. F. Sabirianov, O. Mryasov, M. L. Yan, K. Cho, and D. J. Sellmyer, "Curie temperature of FePt:B2O3 nanocomposite films," *Phys. Rev. B*, vol. 66, pp. 184425-1–184425-6, Nov. 2002.

[4] R. Skomski, "Nanomagnetics," *J. Phys. Condens Matter*, vol. 15, pp. R841–R896, May 2003.

[5] A. B. Shick and O. N. Mryasov, "Coulomb correlations and magnetic anisotropy in ordered $L1_0$ CoPt and FePt alloys," *Phys. Rev. B*, vol. 67, pp. 172407-1–172407-4, May 2003.

[6] R. Skomski and J. M. D. Coey*, Permanent Magnetism*. Bristol: Institute of Physics Publishing, 1999.

[7] R. Skomski, "Phase formation in $L1_0$ magnets," *J. Appl. Phys.*, vol. 101, pp. 09N517-1–09N517-3, May 2007.

[8] A. Kashyap, A. K. Solanki, T. Nautiyal, and S. Auluck, "Effect of pressure on the curie temperature of $\mathrm{Fe_3Pt}$," *Phys. Rev. B*, vol. 52, pp. 13471–13474, Nov. 1995.

[9] J. M. MacLaren, S. Willoughby, M. E. McHenry, B. Ramalingum, and S. G. Sankar, "First principle calculations of the electronic structure of $\mathrm{Fe_{1-x}Co_xPt}$," *IEEE Trans. Magn.*, vol. 37, no. 4, pp. 1277–1279, Jul. 2001.

[10] S. Willoughby, J. MacLaren, T. Ohkubo, S. Jeong, M. E. McHenry, D. E. Laughlin, S.-J. Choi, and S.-J. Kwon, "Electronic, magnetic, and structural properties of $\mathrm{L1_0\ FePt_xPd_{1-x}}$ alloys," *J. Appl. Phys.*, vol. 91, pp. 8822-1–8822-3, May 2002.

[11] P. K. Sahota, Y. Liu, R. Skomski, P. Manchanda, R. Zhang, H. Fangohr, M. Franchin, G. C. Hadjipanayis, A. Kashyap, and D. J. Sellmyer, "Ultrahard magnetic nanostructures," *J. Appl. Phys.*, vol. 111, pp. 07E345-1–07E345-3, Mar. 2012.

[12] Y. Liu, T. A. George, R. Skomski, and D. J. Sellmyer, "Aligned and exchanged-coupled FePt-based films," *Appl. Phys. Lett.*, vol. 99, pp. 172504-1–172504-3, Oct. 2011.

[13] H. Kono, "On ferromagnetic phase in manganese-aluminum system," *J. Phys. Soc. Jpn.*, vol. 13, p. 1444, Aug. 1958.

[14] A. J. J. Koch, P. Hokkeling, M. G. V. D. Sterg, and K. J. DeVos, "New material for permanent magnets on base of Mn and Al," *J. Appl. Phys.*, vol. 31, p. S75, May 1960.

[15] Y. Kurtulus and R. Dronskowski, "Electronic structure, chemical bonding, and spin polarization in ferromagnetic MnAl," *J. Solid State Chem.*, vol. 176, p. 390, Nov. 2003.

[16] , J. E. Evetts, Ed.*, Concise Encyclopedia of Magnetic and Superconducting Materials*. Pergamon: Oxford, 1992.

[17] P. Wasilewski, "Magnetic characterization of new magneti mineral tetrataenite and its contrast with isochemical taenite," *Phys. Earth Planet. Int*, vol. 52, pp. 150–158, 1988.

[18] R. S. Clarke and E. R. D. Scott, "Tetrataenite-ordered FeNi, a new mineral in meteorites," *Amer. Mineral.*, vol. 65, pp. 624–630, 1980.

[19] C.-W. Yang, D. B. Williams, and J. I. Goldstein, "A revision of the Fe-Ni phase diagram at low temperatures ($< 400\,^\circ\mathrm{C}$)," *J. Phase Equilibria*, vol. 17, no. 6, pp. 522–531, 1996.

[20] K. B. Reuter, D. B. Williams, and J. I. Goldstein, "Ordering in the Fe-Ni and Fe-Ni-P systems under electron irradiation," *Metall. Trans. A*, vol. 20, pp. 719–726, Apr. 1989.

[21] M. Z. Dang and D. G. Rancourt, "Simultaneous magnetic and chemical ordered-disordered phenomena in $\mathrm{Fe_3Ni}$, FeNi, and $\mathrm{FeNi_3}$," *Phys. Rev. B*, vol. 53, pp. 2291–2302, Feb. 1996.

[22] L. Néel, J. Pauleve, R. Pauthenet, J. Laugier, and D. Dautreppe, "Magnetic properties of an iron-nickel single crystal ordered by neutron bombardment," *J. Appl. Phys.*, vol. 35, pp. 873-1–873-4, Dec. 1964.

[23] L. H. Lewis, K. Barmak, J. I. Goldstein, F. Pinkerton, and R. Skomski, "Towards stabilization of $L1_0$-type FeNi compounds for permanent magnet applications," in *Proc. REPM'12*, Nagasaki, Japan, 2012, pp. 102–105.

[24] G. Kresse and D. Joubert, "From ultrasoft pseudo potentials to the projector augmented-wave method," *Phys. Rev. B*, vol. 59, pp. 1758–1775, Jan. 1999.

[25] Y. Wang and J. P. Perdew, "Correlation hole of the spin-polarized electron gas, with exact small-wave-vetor ans high-density scaling," *Phys. Rev. B*, vol. 44, pp. 13298–13307, Dec. 1991.

[26] S. H. Vosko, L. Wilk, and M. Nusair, "Accurate spin-dependent electron liquid correlation energies for local spin density calculations: A critical analysis," *Can. J. Phys.*, vol. 58, pp. 1200–1211, 1980.

[27] H. J. Monkhorst and J. D. Pack, "Special points for Brillouin-zone intergrations," *Phys. Rev. B*, vol. 13, pp. 5188–5192, Jun. 1976.

[28] E. G. Moroni, G. Kresse, J. Hafner, and J. Furthmüller*, Ultrasoft Pseudopotentials Applied to Magnetic Fe, Co, and Ni: From Atoms to Solids*, vol. 56, pp. 15629–15646, Jun. 1997.

[29] P. Villars and L. D. Calvert*, Pearson's Handbook of Crystallographic Data for Intermetallic Phase*. Meta Park, OH: ASM, 2000.

[30] J. F. Albertson, G. B. Jensen, and J. M. Knudsen, "Structure of Taenite in two iron meteorites," *Nature*, vol. 273, pp. 453–454, Jun. 1978.

[31] A. Kashyap, R. Skomski, A. K. Solanki, Y. F. Xu, and D. J. Sellmyer, "Magnetism of $L1_0$ compounds with the composition $MT$ ($M =$ Rh, Pd, Pt and $T =$ Mn, Fe, Co, Ni)," *J. Appl. Phys.*, vol. 95, pp. 7480-1–7480-3, Jun. 2004.

[32] G. Brown, B. Kraczek, A. Janotti, T. C. Schulthess, G. M. Stocks, and D. D. Johnson, "Competition between ferromagnetism and antiferromagnetism in FePt," *Phys. Rev. B.*, vol. 68, pp. 052405-1–052405-4, Aug. 2003.

[33] J. M. MacLaren, R. R. Duplessis, R. A. Stern, and S. Willoughby, "First principle calculations of FePt, CoPt, $\mathrm{Co_3Pt}$, and $\mathrm{Fe_3Pt}$ alloys," *IEEE Trans. Magn.*, vol. 41, no. 12, pp. 4374–4379, Dec. 2005.

[34] C. Zhou, T. C. Schulthess, and O. N. Mryasov, "Magnetic aniostropy of FePt nanoparticles: Temperature-dependent free energy barrier for switching," *IEEE Trans. Magn.*, vol. 43, no. 6, pp. 2950–2952, Jun. 2007.

[35] J. Lyubina, I. Opahle, M. Richter, O. Gutfleisch, K.-H. Müller, L. Schultz, and O. Isnard, "Influence of composition and order on the magnetism of Fe-Pt alloys: Neutron powder diffaction and theory," *Appl. Phys. Lett.*, vol. 89, pp. 032506–032509, Jul. 2006.

[36] S. K. Chen, S. N. Hsiao, F. T. Yuan, and W. C. Chang, "Magnetic property enhancement of $\mathrm{Fe_{49-x}Co_xPt_{51}}$ ($x = 0.0$, 0.7, 1.3, 2.2) thin films," *IEEE Trans. Magn.*, vol. 41, no. 10, pp. 3784–3786, Oct. 2005.

[37] A. Sakuma, "Electronic structure and magnetocrystalline anisotropy energy of MnAl," *J. Phys. Soc. Jpn.*, vol. 63, pp. 1422–1428, 1994.

[38] J. H. Park, Y. K. Hong, S. Bae, J. J. Lee, J. Jalli, G. S. Abo, N. Neveu, S. G. Kim, C. J. Choi, and J. G. Lee, "Saturation magnetization and crystalline anisotropy calculations for MnAl permanent magnet," *J. Appl. Phys.*, vol. 107, pp. 09A731-1–09A731-3, Apr. 2010.

[39] L. Ma, D. B. Williams, and J. I. Goldstein, "Determination of the Fe-rich portion of the Fe-Ni-S phase diagram," *J. Phase Equilibria*, vol. 19, no. 4, pp. 299–309, 1998.

[40] I. G. Kabanova, V. V. Sagaradze, and N. V. Kataeva, "Formation of an $L1_0$ superstructure in austenite upon the $\alpha - \gamma$ transformation in the invar alloy Fe–32%Ni," *Phys. Metals Metallogr.*, vol. 112, pp. 267–276, 2011.

[41] P. Ravindran, A. Kjekshus, H. Fjellvåg, P. James, L. Nordström, B. Johansson, and O. Eriksson, "Large magnetocrystalline anisotropy in bilayer transition metal phase from first-principle full-potential calculations," *Phys. Rev. B*, vol. 63, pp. 144409-1–144409-18, Mar. 2001.

[42] C. Mitsumata, Y. Kota, A. Sakuma, and M. Kotsugi, "Magnetic ansiotropy in ordered $\mathrm{L1_0}$type NiFe alloy," *J. Magn. Soc. Jpn.*, vol. 35, pp. 52–55, 2011.